Frizzled6 controls hair patterning in mice

Nini Guo*, Charles Hawkins†, and Jeremy Nathans*‡§¶‖

Departments of *Molecular Biology and Genetics, ‡Neuroscience, and §Ophthalmology, ¶Howard Hughes Medical Institute, and †Transgenic Core Facility, Johns Hopkins University School of Medicine, Baltimore, MD 21205

Contributed by Jeremy Nathans, April 22, 2004

Hair whorls and other macroscopic hair patterns are found in a variety of mammalian species, including humans. We show here that Frizzled6 (Fz6), one member of a large family of integral membrane Wnt receptors, controls macroscopic hair patterning in the mouse. *Fz6* is expressed in the skin and hair follicles, and targeted deletion of the *Fz6* gene produces stereotyped whorls on the hind feet, variable whorls and tufts on the head, and misorientation of hairs on the torso. Embryo chimera experiments imply that Fz6 acts locally to control or propagate the macroscopic hair pattern and that epithelial cells rather than melanocytes are the source of Fz6-dependent signaling. The *Fz6* phenotype strongly resembles the wing-hair and bristle patterning defects observed in *Drosophila frizzled* mutants. These data imply that hair patterning in mammals uses a Fz-dependent tissue polarity system similar to the one that patterns the *Drosophila* cuticle.

The founding member of the Frizzled (Fz) family was identified in *Drosophila* as a gene required for producing the correct orientation of cuticular bristles and hairs, a process referred to as tissue or planar polarity (1, 2). Fz family members have subsequently been found throughout the animal kingdom (3), and experiments in cell culture and in *Drosophila* have shown that they function as Wnt receptors (4–8). Current evidence indicates that Fzs can signal through at least three distinct pathways: the "canonical Wnt pathway" (involving stabilization of β-catenin and selective gene activation), a rho/jun kinase pathway, and a G protein pathway that mobilizes calcium (9). At present, the identity of the ligand(s) involved in tissue polarity signaling is unknown.

Thus far, *in vivo* functions have been defined for only three of the 10 mammalian Fz genes. Loss of *Fz3* produces defects in axonal development and pathfinding in the CNS (10, 11); loss of *Fz4* produces progressive cerebellar degeneration, esophageal enlargement, atrophy of the stria vascularis in the inner ear, and defective development of the retinal vasculature (12–14); and loss of *Fz5* produces defects in yolk sac and placental angiogenesis (15). Whether any of these diverse phenotypes involves the tissue polarity pathway is unclear. However, a bona fide mammalian tissue polarity system almost certainly exists because (*i*) there are mammalian orthologues for most, if not all, of the *Drosophila* genes implicated in tissue polarity, and (*ii*) orientation defects are observed in developing auditory hair cells in mice defective in any of three of these orthologues (*Vangl2, Scrb1*, and *Celsr1*; refs. 16 and 17), and similar defects can be induced by application of soluble Wnt antagonists in explant culture (18).

In this paper, we show that the phenotype associated with targeted mutation in the mouse *Fz6* gene strongly resembles the wing hair and bristle patterning defects observed in *Drosophila fz* mutants. These data imply that hair patterning in mammals uses an Fz-dependent tissue polarity system similar to the one that patterns the *Drosophila* cuticle.

Experimental Procedures

Generation of *Fz6*(−/−) Mice. The *Fz6* knock-in construct deletes codons 1–125 (coding for the signal sequence and most of the cysteine-rich ligand-binding domain), and carries a loxP-flanked *PGK-neo* cassette between the homology arms and a Herpes simplex virus thymidine kinase cassette within the vector. Linearized DNA was electroporated into 129 embryonic stem cells and the cells were grown in medium containing G418 and gancyclovir. Colonies were picked 8 days after plating and screened by Southern blot hybridization. Embryonic stem cell clones carrying the homologously recombined allele were injected into C57BL6 blastocysts. Animal breeding and genotyping were performed by using standard methods. The targeted *Fz6* allele was maintained both on a mixed C57BL6 × 129 background and on a pure 129 background. The loxP-flanked *PGK-neo* cassette was removed by crossing to germ-line cre mice (19).

Generation and Analysis of Chimeric Mice by Embryo Aggregation. Chimeras between ICR *Fz6*(+/+) and C57BL6 × 129 *Fz6*(+/−) or *Fz6*(−/−) were generated by using standard embryo aggregation methods (20). At approximately postnatal day (P)10, mice were photographed and the skin from the sides and dorsal surface of each hind foot was dissected in one piece, flattened, mounted on a Sylgard block with insect pins, and photographed before and after 5-bromo-4-chloro-3-indolyl β-D-galactoside (X-Gal) staining. In a subset of animals, the skin from the head and back was similarly analyzed.

Antibody Production and Purification. A synthetic peptide corresponding to the C-terminal 17 aa of mouse Fz6 with an additional cysteine added at the N terminus (CSASRARKEQGAGSHSDA) was crosslinked with glutaraldehyde to BSA (21) and was used to immunize rabbits. Antisera were affinity-purified by using the same peptide coupled to an Affi-Gel 10 matrix (Bio-Rad).

Immunoblotting. Skin from the back of P1 mice was homogenized in 50 mM Tris·HCl, pH 7.5/150 mM NaCl/1 mM EDTA/1% SDS/protease inhibitors. Extracts were centrifuged at 7,000 × *g* for 5 min at 4°C. Supernatant proteins were resolved by SDS/PAGE and were probed with affinity-purified anti-Fz6 antibodies.

X-Gal Histochemistry. X-Gal staining was performed overnight at 37°C on the following embryos or tissues in standard X-Gal staining solution (22) supplemented with 0.02% Tween 20: (*i*) embryonic day (E)14.5 embryos that were immersion fixed for 3 h at 4°C in PBS, 0.5% glutaraldehyde; (*ii*) E16.5 embryos or P1 mice that were freshly frozen, cryosectioned at 10 μm, and postfixed in PBS, 0.5% glutaraldehyde for 10 min at room temperature; and (*iii*) skin dissected from dorsal hind feet and head from chimeric mice, and postfixed in PBS, 0.5% glutaraldehyde for 40 min at room temperature. No differences in the pattern of X-Gal staining were observed between mice that

Abbreviations: Fz, Frizzled; X-Gal, 5-bromo-4-chloro-3-indolyl β-D-galactoside; P*n*, postnatal day *n*; E*n*, embryonic day *n*; nLacZ, a nuclear localized derivative of *Escherichia coli* β-galactosidase.

See Commentary on page 9173.

‖To whom correspondence should be addressed at: 805 Preclinical Teaching Building, 725 North Wolfe Street, Johns Hopkins University School of Medicine, Baltimore, MD 21205. E-mail: jnathans@jhmi.edu.

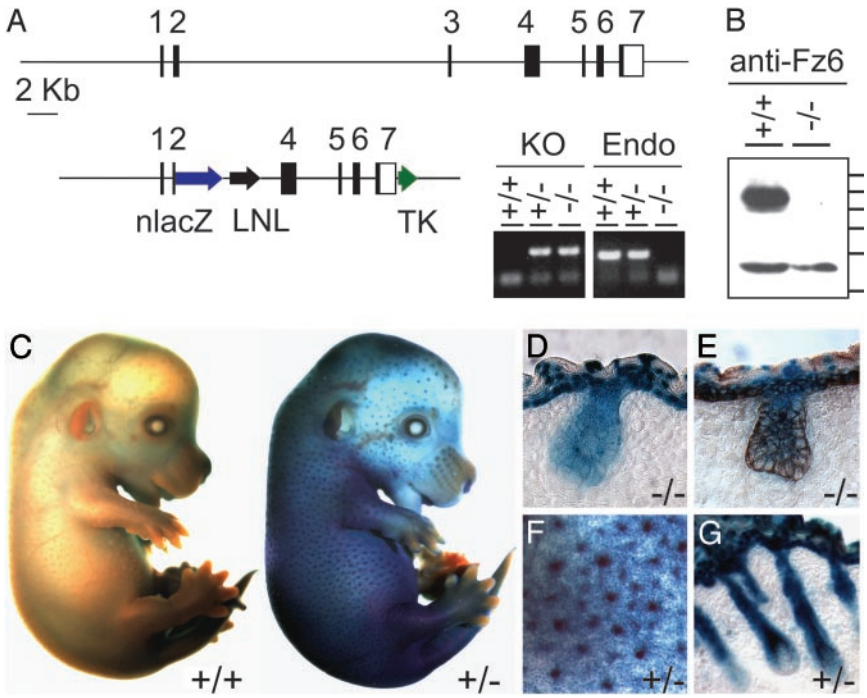

Fig. 1. Targeted mutation of the *Fz6* gene and expression of *Fz6-nlacZ* in skin and hair follicles. (*A Upper*) Structure of the *Fz6* locus. Black rectangles represent the seven exons; in exons 2–7, the shaded areas represent the *Fz6* coding region. (*Lower Left*) Targeting vector. LNL, *PGK-neo* gene flanked by loxP sites; TK, herpes simplex virus thymidine kinase cassette. (*Right*) Genotyping of tail DNA with PCR primers specific for the *neo-Fz6* junction (KO) or endogenous *Fz6* sequences deleted in the targeted allele (Endo). (*B*) Immunoblot of proteins from P1 skin probed with affinity-purified antibodies directed against the C-terminal 17 aa of Fz6. A band of ≈85 kDa is present in the *Fz6*(+/+) sample and absent in the *Fz6*(−/−) sample and is presumed to be Fz6; a crossreacting band of ≈55 kDa is seen in both samples. Protein molecular mass standards from top to bottom are 100, 90, 80, 70, 60, and 50 kDa. (*C*) X-Gal stain of E14.5 embryos. (*Left*) *Fz6*(+/+). (*Right*) *Fz6*(+/−). (*D* and *E*) X-Gal stain of *Fz6*(−/−) skin at E16.5; in *E*, a similar section has also been immunostained for keratin-14 (brown). X-Gal staining is present in the periderm, epidermis, and hair follicles. (*F*) Enlarged image of the flank of the *Fz6*(+/−) embryo in *C* shows X-Gal stain concentrated in developing hair follicles. (*G*) X-Gal stain of *Fz6*(+/−) skin at ≈P1. *C–G* show strong expression of the *Fz6-nlacZ* reporter in developing epidermis and hair follicles. *Fz6*(+/−) and *Fz6*(−/−) show the same pattern of X-Gal staining.

retained the loxP-flanked *PGK-neo* cassette or from which the cassette had been excised by cre recombinase.

Immunohistochemistry. Immunostaining was performed on skin sections prestained with X-Gal. Reagents were obtained from the following sources: anti-mouse keratin 14 polyclonal antibody (Covance, Denver, PA), biotinylated goat anti rabbit IgG (Vector Laboratories), and extravidin-peroxidase conjugate (Sigma).

Histochemistry. Hematoxylin/eosin staining was performed by using standard methods. For P3 mice, the hind feet were freshly frozen, cryosectioned at 10 μm, and postfixed in PBS, 4% PFA for 10 min at room temperature, and stained.

***In Situ* Hybridization.** *In situ* hybridization was performed essentially as described (23) by using unfixed cryosectioned tissue with antisense and sense strand riboprobes synthesized from mouse Sonic hedgehog cDNA.

Results

***Fz6-nlacZ* Expression Pattern.** As part of an effort to systematically define the *in vivo* role(s) of each mammalian Fz gene, we constructed a presumptive null allele of *Fz6*, in which a nuclear localized derivative of *Escherichia coli* β-galactosidase (nLacZ) is expressed under the control of the *Fz6* promoter (Fig. 1 *A* and *B*). Histochemical analysis of tissues in *Fz6*(+/−) and *Fz6*(−/−) animals revealed expression of the *nlacZ* reporter in the skin and vasculature (Fig. 1 *C–G* and data not shown). In postnatal skin, strong expression was found in the epidermis and hair follicles. *Fz6-nlacZ* expression in the developing skin was detected at approximately E11, and expression in presumptive hair follicle precursors was first detected at approximately E13. In mature hair follicles, *Fz6-nlacZ* expression persists along the length of the follicle but is below the limit of detection in melanocytes and the dermal papilla.

Hair Patterns in *Fz6*(−/−) Mice. *Fz6*(−/−) mice are viable and fertile, and appear to be in good health. However, close examination revealed distinctive alterations in hair patterning over much of the body surface (Fig. 2). In WT mice, the hair on the dorsal surface of the feet is oriented toward the digits, and the hair on the dorsal surface of the head and back is oriented caudally. Among >100 *Fz6*(−/−) mice examined to date, the hair on the front feet is oriented normally but a single hair whorl is present on each of the hind feet, clockwise on the right foot, and counterclockwise on the left foot (Fig. 2 *A–D*). On a mixed C57BL6 × 129 background, ≈30% of *Fz6*(−/−) mice have severely aberrant hair patterns on the dorsal surface of the head (Fig. 2 *G–N*); milder aberrations in hair patterning are seen in the remaining *Fz6*(−/−) mice. The patterns include whorls, which are formed by hairs with a divergent orientation (e.g., Fig. 2 *I* and *N*), and tufts or ridges, which are formed by hairs with a convergent orientation (e.g., Fig. 2 *K* and *M*). On the same genetic background, the hair on the back is partly reoriented toward the midline in >95% of *Fz6*(−/−) mice (Fig. 2 *O* and *P*). The hair on the chest, which is arranged in two symmetric whorls in the WT (clockwise on the left and counterclockwise on the right), is variably rearranged (Fig. 2 *S* and *T*). Fig. 2*T* shows a *Fz6*(−/−) mouse with a single and more centrally located chest whorl. Whereas the hair patterns are most clearly seen at approximately P8–P11 when the hair is still relatively short (Fig. 2 *A–D* and *G–R*), they clearly persist in older animals (Fig. 2 *S–V*). Some differences in the *Fz6*(−/−) phenotype are seen on a pure 129 background as compared with a mixed C57BL6 × 129 background; in particular, on the pure 129 background, the hair on the back and flank shows greater deviations from the WT pattern (Fig. 2 *Q* and *R*), and the frequency of severe pattern aberrations on the head is increased to ≈80%. Within the same breeding colonies, no hair patterning anomalies have been observed among >60 *Fz6*(+/−) or *Fz6*(+/+) mice examined to date, and in the descriptions that follow we will therefore consider *Fz6*(+/−) and *Fz6*(+/+) as equivalently representative of the WT phenotype.

The unusual hair patterns in *Fz6*(−/−) mice do not appear to arise from differences in hair density, as is seen, for example, in the crowded and misoriented hair of transgenic mice that overproduce LEF-1 or a stabilized β-catenin under the control of a *keratin-14* promoter (24, 25). Light microscopic examination

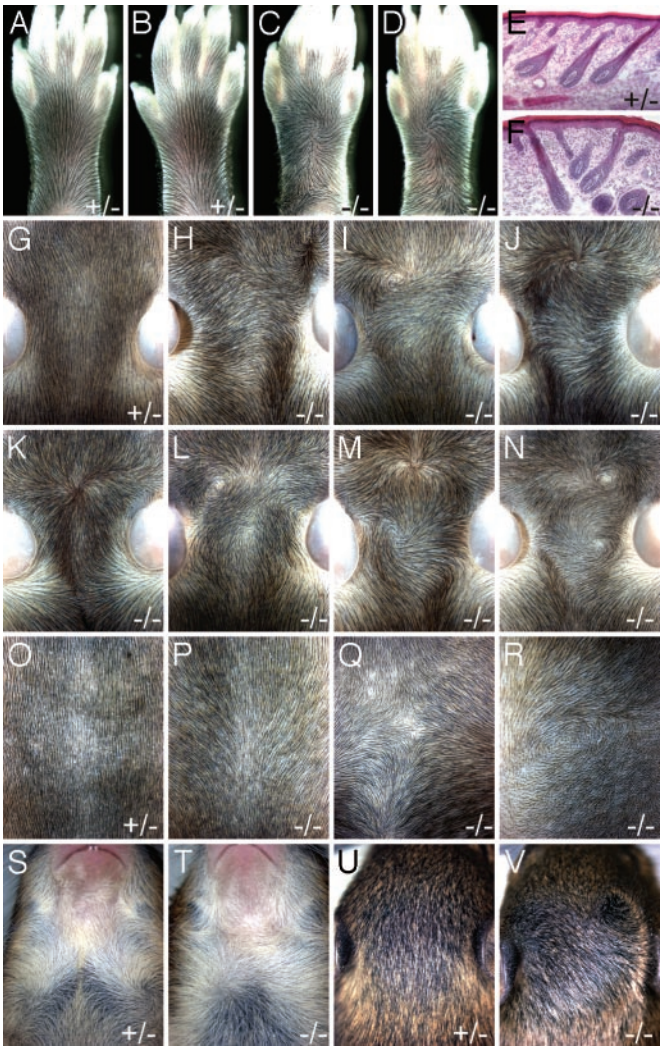

Fig. 2. Altered hair patterns in *Fz6*(−/−) mice. (*A–D*) WT and *Fz6*(−/−) hind feet at approximately P11. (*A* and *C*) Left feet. (*B* and *D*) Right feet. (*E* and *F*) Hematoxylin/eosin staining of frozen sections of skin on the dorsal surface of the hind foot at approximately P3 shows that *Fz6*(−/−) hair follicles exhibit normal morphology, but, in regions of aberrant patterning (shown in *F*), they are arranged in divergent orientation. (*G–N*) Hair on the dorsal surface of the head at approximately P9 shows the heterogeneity of hair patterning among *Fz6*(−/−) mice. The ears are seen at the lateral edges of each image; rostral is toward the top. (*O–R*) Hair on the back at approximately P8 shows a rostral to caudal orientation in WT (*O*), a uniform deviation toward the midline in *Fz6*(−/−) on a mixed C57BL6 × 129 background (*P*), and variable deviations on a pure 129 background (*Q* and *R*), including a whorl in *R*. Rostral is toward the top. (*S* and *T*) Hair whorls on the neck and chest at approximately P13. The pair of whorls in *S* is invariant among WT mice. Among *Fz6*(−/−) mice, the pattern is variable. (*U* and *V*) Hair on the dorsal surface of the head at approximately P13. In older mice, longer hair makes the altered hair pattern less apparent.

of the structure of individual *Fz6*(−/−) hair follicles during development and in adulthood showed apparently normal morphology, including growth at an angle to the skin surface (Fig. 2 *E* and *F*) and polarized expression of *Sonic hedgehog* in the hair matrix (data not shown). As expected from their appearance in flatmounts, hair follicles in regions of aberrant patterning (e.g., the center of a whorl) do not conform to the parallel arrangement of neighboring follicles that characterize nearly all regions of the WT coat (Fig. 2 *E* and *F*). In *Fz6*(−/−) mice at P1, cochlear hair cells exhibit the normal orientation of stereocilia in both the C57BL6 × 129 and the pure 129 backgrounds (data not shown).

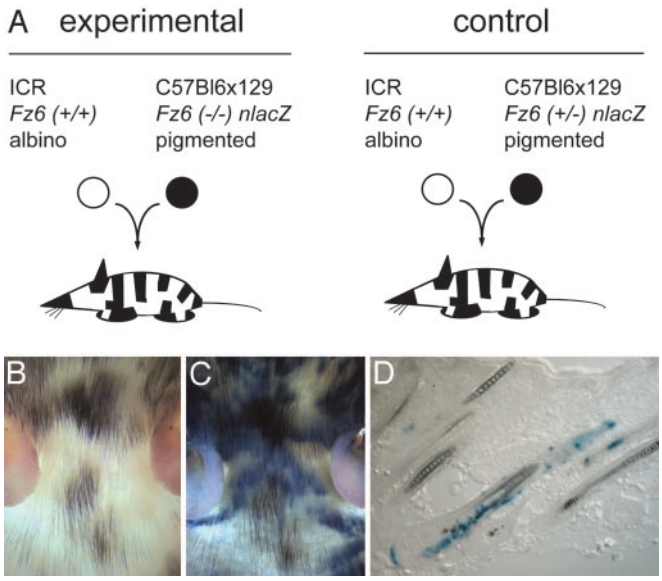

Fig. 3. Generation of chimeric mice. (*A*) Diagram of the experimental (*Left*) and control (*Right*) embryo aggregation protocols. (*B* and *C*) Unstained (*B*) and X-Gal-stained (*C*) flatmounts of skin from the head of an albino ICR *Fz6*(+/+):pigmented C57BL6 × 129 *Fz6*(−/−) chimeric mouse at approximately P10 shows the independent patterns of tissue chimerism for epidermal cells (X-Gal-stained or unstained) and melanocytes (pigmented or albino). A small amount of tissue shrinkage accompanies the fixation and X-Gal staining procedure. (*D*) An X-Gal-stained frozen section from the abdomen of a chimeric mouse shows the characteristic heterogeneity of *Fz6*(−/−) epidermal cells (X-Gal-stained) within single hair follicles. This image also shows, on the scale of individual hair follicles, the independent patterns of tissue chimerism for epidermal cells and melanocytes.

***Fz6*(−/−):*Fz6*(+/+) Embryo Chimeras.** In *Drosophila*, the analysis of genetic mosaics demonstrated that *fz* acts locally to determine cuticular polarity. Patterning defects in the wing were observed in *fz*(−/−) tissue patches and in a small zone of genetically WT cells immediately adjacent to the mutant patch (1, 26). The interpretation of these experiments is facilitated by the simple structure of the *Drosophila* wing blade, which consists of an epithelial monolayer where each cell elaborates a single polarized hair. Mammalian hair development is more complex, because each hair follicle is specified by a series of interactions between mesenchymal and epithelial cells, both of which contribute to the mature follicle (27). Melanoblasts derived from migrating neural crest cells are also present from the earliest times of hair follicle development and become an integral part of the follicle. To determine the extent to which Fz6 acts locally in hair patterning and to assess the effect on hair patterning of the relative densities of *Fz6*(−/−) and *Fz6*(+/+) epithelial cells, we studied chimeras created by aggregation of albino ICR *Fz6*(+/+) and pigmented C57BL6 × 129 *Fz6*(−/−) embryos (Fig. 3*A*). The different pigmentation phenotypes of the two lines also permitted an experimental test of the possible involvement of melanocytes in Fz6-dependent hair patterning. This possibility was suggested by the observation that cranial neural crest cells play a central role in patterning of bone, cartilage, and soft tissues in the developing head (28).

Among 31 mice obtained from albino ICR *Fz6*(+/+):pigmented C57BL6 × 129 *Fz6*(−/−) embryo aggregation and examined at approximately P10, 30 were clearly chimeric based on hair pigmentation and/or X-Gal staining. In this experiment, pigmentation marks melanocytes derived from *Fz6*(−/−) embryos, and the X-Gal stain marks *Fz6*(−/−) epidermis and hair follicles. For each animal, the head, back, and hind feet were first analyzed for hair orientation and pigmentation, and were then

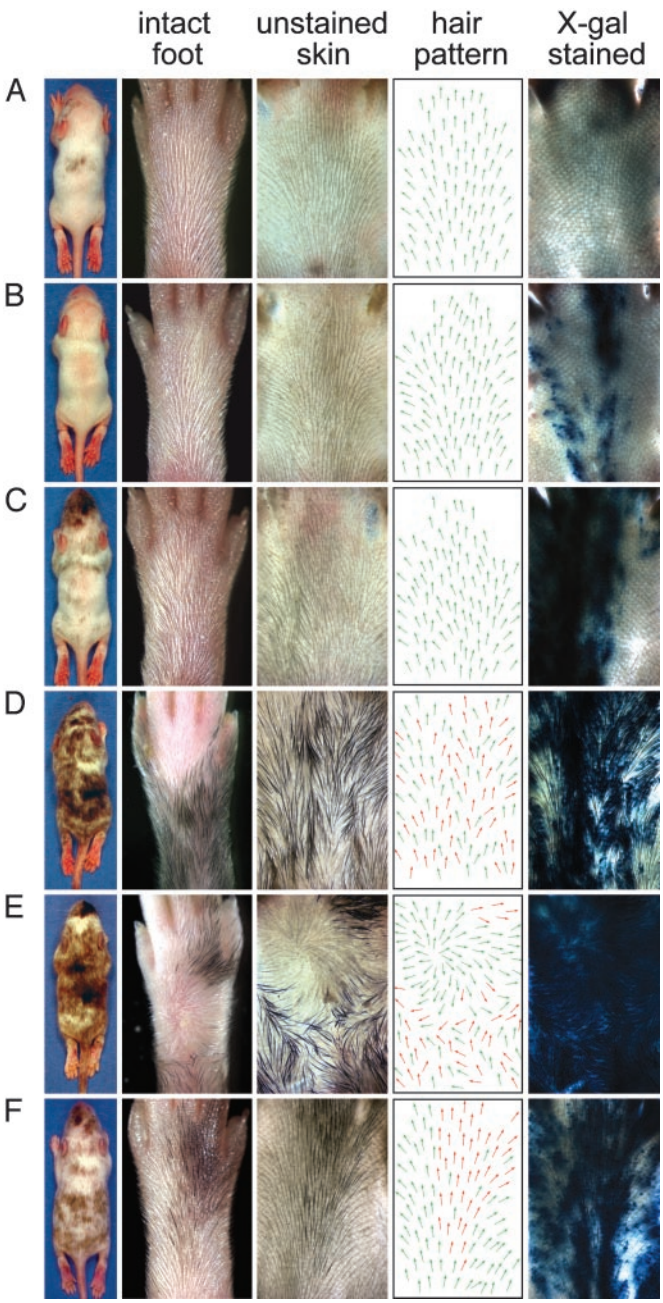

Fig. 4. Hair patterns in embryo aggregation chimeras at approximately P10. From left to right, each horizontal row shows a chimeric mouse, the dorsal surface of one of its hind feet, an unstained flatmount of skin from that foot, a diagram of the unstained flatmount in which each arrow indicates the local hair orientation, and the same flatmount after X-Gal staining. In the diagrams of hair orientation, green and red arrows represent the approximate contributions of albino and pigmented hair, respectively. (*A–E*) Albino ICR *Fz6*(+/+):pigmented C57BL6 × 129 *Fz6*(−/−) chimeras with, from top to bottom, increasing contributions of *Fz6*(−/−) tissue. (*F*) A control albino ICR *Fz6*(+/+):pigmented C57BL6 × 129 *Fz6*(+/−) chimera shows roughly equal contributions of WT and *Fz6*(+/−) tissue but exhibits a WT hair pattern. The small boundary of misaligned hairs at lower left in the flatmount in *B* and at lower right of the flatmount in *F* is an artifact that arises from flattening the highly curved skin at the lateral edge of the foot.

Fig. 5. Hair patterns among mammals. (*A–D*) Hair whorls in humans. (*A*) Single occipital whorl. (*B*) Frontal whorl with an upsweep of the frontal hair on the opposite side of the forehead. The brother of this subject has the same hair pattern. (*C* and *D*) Double occipital whorls in a father (*C*) and son (*D*). (*E* and *F*) Hair patterns in horses. (*E*) Most horses have a single whorl between the eyes; an analogous whorl is present in cattle. (*F*) Hair pattern on the flank at the junction of the hind leg (on the left) and torso (on the right). (*G* and *H*) Hair patterns in guinea pigs. Prominent whorls over the surface of the body (*G*) are referred to as rosettes. (*I*) In dogs, complex hair patterns are typically present on the upper chest; shown are symmetric whorls on the chest of a Chihuahua. (*J*) American prairie dog showing one of the two bilaterally symmetric whorls on the upper chest. *G*, *H*, and *J* are reprinted from refs. 36–38, respectively.

subjected to X-Gal staining. Fig. 4 *A–E* shows examples of this analysis for the hind feet, a region in which the *Fz6*(−/−) phenotype is distinctive and shows minimal animal-to-animal variability. Among individual mice there was a rough correlation between the percent of the skin surface that was occupied by pigmented hair and the percent that was X-Gal stained, both of which reflect the overall contribution of *Fz6*(−/−) tissue to the chimera. However, the patterns and locations of pigmented hair and X-Gal-stained skin were not correlated, as expected from the distinct embryonic origins of melanocytes and skin epithelial cells (Figs. 3 *B* and *C* and 4 *B–E*).

Examination of chimeric hind feet showed that the hair patterning ranges from normal (Fig. 4*A*) to mildly affected (Fig. 4*B*) to severely affected over part (Fig. 4*C*) or most (Fig. 4 *D* and *E*) of the surface. There is a clear correlation between the location and severity of the hair patterning defects and the location and number (or density) of X-Gal-stained epithelial cells (e.g., Fig. 4 *B* and *C*). By contrast, there is little or no correlation between patterning defects and hair pigmentation. For example, Fig. 4 *B* and *C* show disorganized hair patterns in feet with no pigmentation, and Fig. 4*E* shows the most severe phenotype, a full whorl, in a region lacking pigmentation. Reciprocally, in the several chimeric feet with regions of pigmentation where there was little or no X-Gal staining, the hair orientation was largely normal (data not shown). In a control experiment (Fig. 3*A*), 11 chimeras produced by aggregation of albino ICR *Fz6*(+/+) embryos and pigmented C57BL6 × 129 *Fz6*(+/−) embryos showed no deviations from the WT hair pattern (Fig. 4*F*), indicating that the disorganization in hair patterning observed in the *Fz6*(+/+):*Fz6*(−/−) chimeras did not arise from the juxtaposition of ICR and C57BL6 × 129 tissues. Taken together, these data imply that Fz6 acts locally to control or propagate the macroscopic hair pattern and that

epithelial cells rather than melanocytes are the source of Fz6-dependent signaling.

In contrast to the contiguous zones of mutant tissue typically observed in genetic mosaics in *Drosophila*, flatmounts of the skin of *Fz6*(+/+): *F26* (−/−) chimeric mice frequently show interspersion of WT and mutant epithelial cells, and, in cross-section, individual hair follicles are frequently observed to contain both *Fz6*(+/+) and *Fz6*(−/−) cells (Fig. 3*D*). Interestingly, even in chimeras with a large fraction of mutant tissue, the hair patterns generally appear as local irregularities rather than whorls (Fig. 4*D*), and complete whorls were seen on only 2/60 hind feet (Fig. 4*E*). These observations suggest that even a small number of *Fz6*(+/+) cells adjacent to or interspersed with *Fz6*(−/−) cells can, in most cases, disrupt the development of a whorl. It is intriguing that the greatest degree of disorganization in the hair pattern of chimeric mice occurs in regions in which *Fz6*(+/+) and *Fz6*(−/−) epidermal cells are interspersed (e.g., Fig. 4*D*), whereas epidermis that is either uniformly WT or mutant is characterized by a high degree of local order.

Discussion

The present work establishes Fz6 as an essential component of a hair-patterning pathway in mice. The aberrant hair patterns in *Fz6*(−/−) mice do not exhibit a complete randomization of orientation, but instead show a local ordering, with the orientations of neighboring hairs showing a high correlation. Local order is also seen in the bristles and hairs in many of the *Drosophila* tissue polarity mutants and this occurrence leads to macroscopic patterns similar to those of *Fz6*(−/−) mice (1, 29). In *Drosophila*, current evidence suggests that this local order may reflect the assembly of signaling complexes that relay polarity information between the proximal and distal faces of adjacent cells (30). In the mouse, the large distance between adjacent hair follicles, even at early stages of development, suggests the possibility of a more complex mechanism of signal propagation.

Complex hair patterns are prevalent in a variety of mammals, including guinea pigs, prairie dogs, horses, pigs, cattle, dogs, and humans (Fig. 5). Moreover, in many species, including our own, individual variation in hair patterning is well documented (31, 32). The classic studies of Sewall Wright (33) demonstrated the Mendelian nature of hair pattern variations in guinea pigs, and current evidence suggests that genetic factors may also be relevant in humans (e.g., Fig. 5 *C* and *D* and refs. 32 and 34). The present work suggests that natural variation in these patterns, both within and between species, may arise from sequence variation in the genes involved in tissue polarity signaling, including *Fz6*. Interestingly, a recent study (35) has provided evidence for a link between handedness and the orientation of hair whorls on the scalp, suggesting the possibility that the same system that patterns hair may also play a role in left-right asymmetry in the brain.

We thank Philip Smallwood for screening BAC libraries; Jennifer Macke and Yanshu Wang for identifying λ Fz6 genomic clones; Alain Dabdoub, Pierre Coulombe, Mitra Cowan, Sejin Lee, Chunqiao Liu, Xuemei Tong, and Yanshu Wang for advice and reagents; Tudor Badea, Pierre Coulombe, Sejin Lee, Tong Li, Chinqao Liu, Wenqin Luo, Tom Rotolo, Amir Rattner, Randy Reed, David Valle, Yanshu Wang, and Qiang Xu for helpful comments on the manuscript; and Dillon Press, Gloucester Press, and Harper Collins for the use of Fig. 5 *J*, *G*, and *H*, respectively. This work was supported by the Howard Hughes Medical Institute.

1. Gubb, D. & Garcia-Bellido, A. (1982) *J. Embryol. Exp. Morphol.* **68,** 37–57.
2. Vinson, C. R., Conover, S. & Adler, P. N. (1989) *Nature* **338,** 263–264.
3. Wang, Y., Macke, J. P., Abella, B. S., Andreasson, K., Worley, P., Gilbert, D. J., Copeland, N. G., Jenkins, N. A. & Nathans, J. (1996) *J. Biol. Chem.* **271,** 4468–4476.
4. Bhanot, P., Brink, M., Samos, C. H., Hsieh, J. C., Wang, Y., Macke, J. P., Andrew, D., Nathans, J. & Nusse, R. (1996) *Nature* **382,** 225–230.
5. Bhanot, P., Fish, M., Jemison, J. A., Nusse, R., Nathans, J. & Cadigan, K. M. (1999) *Development (Cambridge, U.K.)* **126,** 4175–4186.
6. Kennerdell, J. R. & Carthew, R. W. (1998) *Cell* **95,** 1017–1026.
7. Chen, C. M. & Struhl, G. (1999) *Development (Cambridge, U.K.)* **126,** 5441–5452.
8. Muller, H., Samanta, R. & Wieschaus, E. (1999) *Development (Cambridge, U.K.)* **126,** 577–586.
9. Strutt, D. (2003) *Development (Cambridge, U.K.)* **130,** 4501–4513.
10. Wang, Y., Thekdi, N., Smallwood, P. M., Macke, J. P. & Nathans, J. (2002) *J. Neurosci.* **22,** 8563–8573.
11. Lyuksyutova, A. I., Lu, C. C., Milanesio, N., King, L. A., Guo, N., Wang, Y., Nathans, J., Tessier-Lavigne, M. & Zou, Y. (2003) *Science* **302,** 1984–1988.
12. Wang, Y., Huso, D., Cahill, H., Ryugo, D. & Nathans, J. (2001) *J. Neurosci.* **21,** 4761–4771.
13. Robitaille, J., MacDonald, M. L., Kaykas, A., Sheldahl, L. C., Zeisler, J., Dube, M. P., Zhang, L. H., Singaraja, R. R., Guernsey, D. L., Zheng, B., *et al.* (2002) *Nat. Genet.* **32,** 326–330.
14. Xu, Q., Wang Y., Dabdoub, A., Smallwood, P., Williams, J., Woods, C., Kelley, M., Jiang, L., Tasman, W., Zhang, K. & Nathans, J. (2004) *Cell* **116,** 883–895.
15. Ishikawa, T., Tamai, Y., Zorn, A. M., Yoshida, H., Seldin, M. F., Nishikawa, S. & Taketo, M. M. (2001) *Development (Cambridge, U.K.)* **128,** 25–33.
16. Montcouquiol, M., Rachel, R. A., Lanford, P. J., Copeland, N. G., Jenkins, N. A. & Kelley, M. W. (2003) *Nature* **423,** 173–177.
17. Curtin, J. A., Quint, E., Tsipouri, V., Arkell, R. M., Cattanach, B., Copp, A. J., Henderson, D. J., Spurr, N., Stanier, P., Fisher, E. M., *et al.* (2003) *Curr. Biol.* **13,** 1129–1133.
18. Dabdoub, A., Donohue, M. J., Brennan, A., Wolf, V., Montcouquiol, M., Sassoon, D. A., Hseih, J. C., Rubin, J. S., Salinas, P. C. & Kelley, M. W. (2003) *Development (Cambridge, U.K.)* **130,** 2375–2384.
19. Schwenk, F., Baron, U. & Rajewsky, K. (1995) *Nucleic Acids Res.* **23,** 5080–5081.
20. Maatman, R., Gertsenstein, M., de Meijer, E., Nagy, A. & Vintersten, K. (2003) *Methods Mol. Biol.* **209,** 201–230.
21. Harlow, E. & Lane, D. (1988) in *Antibodies: A Laboratory Manual* (Cold Spring Harbor Lab. Press, Plainview, NY), pp. 726.
22. Wang, Y., Macke, J. P., Merbs, S. L., Zack, D. J., Klaunberg, B., Bennett, J., Gearhart, J. & Nathans, J. (1992) *Neuron* **9,** 429–440.
23. Schaeren-Wiemers, N. & Gerfin-Moser, A. (1993) *Histochemistry* **100,** 431–440.
24. Zhou, P., Byrne, C., Jacobs, J. & Fuchs, E. (1995) *Genes Dev.* **9,** 700–713.
25. Gat, U., DasGupta, R., Degenstein, L. & Fuchs, E. (1998) *Cell* **95,** 605–614.
26. Vinson, C. R. & Adler, P. N. (1987) *Nature* **329,** 549–551.
27. Hardy, M. H. (1992) *Trends Genet.* **8,** 55–61.
28. Santagati, F. & Rijli, F. M. (2003) *Nat. Rev. Neurosci.* **4,** 806–818.
29. Adler, P. N. (1987) *Dev. Genet. (Amsterdam)* **8,** 99–119.
30. Axelrod, J. D. (2001) *Genes Dev.* **15,** 1182–1187.
31. Nordby, J. E. (1932) *J. Hered.* **23,** 397–404.
32. Samlaska, C. P. (1989) *J. Am. Acad. Dermatol.* **21,** 553–556.
33. Wright, S. (1950) *J. Exp. Zool.* **113,** 33–63.
34. Kiil, V. (1948) *J. Hered.* **39,** 206–216.
35. Klar, A. J. (2003) *Genetics* **165,** 269–276.
36. Petty, K. (1989) *Guinea Pigs* (Gloucester Press, New York).
37. Taylor, D. (1996) *Small Pet Handbook* (Harper Collins, Hauppauge, NY).
38. Beers, D. S. (1990) *The Prairie Dog* (Dillon Press, Minneapolis).